Magnetization Reversal in Arrays of Perpendicularly Magnetized Ultrathin Dots Coupled by Dipolar Interaction

T. Aign,[1,*] P. Meyer,[1] S. Lemerle,[1] J. P. Jamet,[1] J. Ferré,[1] V. Mathet,[2] C. Chappert,[2] J. Gierak,[3] C. Vieu,[3] F. Rousseaux,[3] H. Launois,[3] and H. Bernas[4]

[1]*Laboratoire de Physique des Solides, URA CNRS 002, Université Paris-Sud, 91405 Orsay, France*

[2]*Institut d'Electronique Fondamentale, URA CNRS 022, Université Paris-Sud, 91405 Orsay, France*

[3]*Laboratoire de Microstructures et de Microélectronique, UPR CNRS 020, 196 Avenue Henry Ravera, BP107, 92225 Bagneux, France*

[4]*Centre de Spectrométrie Nucléaire et de Spectrométrie de Masse, UPR CNRS 6412, Université Paris-Sud, 91405 Orsay, France*

(Received 29 July 1998)

Arrays of micron size perpendicularly magnetized ultrathin Co dots with 20 nm separation were obtained using ion irradiation by a focused ion beam and studied by polar magneto-optical microscopy. Because irradiation induces easy nucleation regions along dot borders, magnetization reversal inside the dots under a perpendicular field is due only to domain wall propagation, driven by applied field and dipolar interactions. Frustrated checkerboard patterns are observed in the demagnetized state, in agreement with numerical simulations. This opens the way to experimental studies on model arrays of interacting Ising dots. [S0031-9007(98)07995-2]

PACS numbers: 75.70.Ak, 05.50.+q, 61.80.Jh, 75.70.Kw

Gaining a precise control of the magnetization reversal processes in submicron magnetic structures is a key issue for future applications to spin electronic devices or ultrahigh density recording media. Dipolar interaction will be a crucial parameter in densely packed systems. We shall restrict ourselves here to the case of samples magnetized out of plane, for which large differences between the applied and the internal fields have been predicted due to dipolar coupling [1]. In granular media, the study is made difficult by the competition between exchange and dipolar interactions and the usually wide distributions of crystallographic and magnetic local parameters. For instance, in the archetypal CoCr films developed for perpendicular recording [1,2], the exchange interaction between columnar crystallites is too large and widely distributed to allow a precise investigation of dipolar coupling effects. A better model system is that of Fe needles grown in a regular alumite array. The effect of nonuniformity of the demagnetizing field in the array during reversal has been emphasized in that case [3]. However, local topological inhomogeneities prevented interpretation of the data in full detail [4]. A better control of the geometrical parameters can be realized using high resolution lateral patterning of homogeneous thin magnetic films [5]. To our knowledge, only one team [6,7] has studied the magnetic switching of dipolar interacting Ising dots with out-of-plane anisotropy under a perpendicular applied field; this was for a regular 2D array of large garnet pixels. The magnetic switching of a given pixel was found to depend on the magnetic configuration of the surrounding ones. However, the large dispersion of coercive fields from pixel to pixel prevented the deduction of valuable information on their collective behavior. A similar dispersion of coercive fields was observed in patterned arrays of Au/Co/Au(111) sandwiches [8]. Even starting from high quality films, where magnetization reverses through uniform domain wall (DW) propagation [9], a large distribution of coercive fields is obtained in dot arrays due to the initial distribution of nucleation fields, which is sampled by the patterning process [8].

We report here the first comprehensive study of the perpendicular in-field magnetization reversal of patterned arrays of dipolar coupled Ising dots. Using an original patterning method based on ion irradiation with a focused ion beam (FIB) system, we were able to fabricate for the first time arrays of magnetostatically coupled micron size Ising dots with very small coercive field dispersion. Polar magneto-optical (MO) microscopy allowed us to evidence the influence of dipolar interaction on the magnetization reversal in individual dots and on the collective behavior of the array. From comparison with numerical simulations we were then able to clearly identify the relevant parameters.

Our initial magnetic film is a highly uniform Pt(3.4 nm)/Co(1.4 nm)/Pt(4.5 nm) sandwich structure, epitaxially grown using magnetron sputtering on a transparent $Al_2O_3(0001)$ single crystal substrate. We adapted a preparation method originally optimized for UHV deposition [10]. As grown films exhibit perpendicular magnetization up to a Co thickness of 2.2 nm. The magnetization reversal is dominated by easy DW propagation [11] following rare nucleation events, as expected for high quality Co/Pt films [12]. The Co layer thickness of 1.4 nm chosen for this study, well below the spin reorientation critical thickness, preserves a large perpendicular magnetic anisotropy while being thick enough to provide strong dipolar effects between dots and large magneto-optical effects required for our high resolution (0.5 μm) MO microscopy studies [9].

Two arrays of 80×80 rectangular ($1.35\ \mu\text{m} \times 1\ \mu\text{m}$) dots were patterned on the same sample using

 0031-9007/98/81(25)/5656(4)$15.00

FIB bombardment with Ga^+ ions at 28 keV. In previous work, we have shown that magnetic properties (coercivity, anisotropy, Curie temperature) of Pt/Co/Pt films can be reduced in a controlled way by uniform 25 keV He^+ ion irradiation [13]. Although the nature of the irradiation induced structural modifications is different with 28 keV Ga^+ ions, a similar controlled reduction of magnetic properties is observed. For this work, the separation between dots was obtained by drawing lines of exposure points with 4.6 nm steps. The dwell time at each point is different for the two arrays, corresponding to line doses of, respectively, 1.09 nC/cm (low dose array, or LDA) and 3.26 nC/cm (high dose array, or HDA). The full width at half maximum of the focused beam diameter is 30 to 50 nm, but since penetrating Ga^+ ions create defect cascades, the damaged zones around exposure points in the magnetic layer are larger. Along the line, due to the small distance between points the damage profile is uniform, while across the lines it can be assumed to be Gaussian [14], with a total width which is the sum of the beam diameter and the lateral damage straggling (about 15 nm). This creates a spatial variation of local magnetic properties such as the magnetic anisotropy and the Curie temperature. From comparison with uniformly irradiated samples, we estimate that the central part (about 20 nm for LDA and 30 nm for HDA) of the lines becomes paramagnetic at room temperature. The irradiation is thus efficient enough to break the exchange interaction between dots. Moreover, local anisotropy and Curie temperature rise when going away from the line center. Given the rather large extension of the damage profile, we can define "local" values of nonlocal parameters like the nucleation and domain wall propagation fields. These will be much reduced along the dot borders, while inside the dot the local DW propagation field [15] H_p of the as grown film ($H_p > 300$ Oe) should be preserved.

We have calculated the profile inside a dot of the demagnetizing field H_d due to a uniformly magnetized surround array. As expected, H_d favors the switching of dots and reaches large negative values at their edges, especially at corners. Using geometrical and magnetic parameters of the LDA, H_d is found to be nearly constant and equal to -25 Oe over the central zone of the dot and takes values about 4 times larger at its boundaries. Hence, in zero field the weakly magnetic areas around the dots will reverse their magnetization in the dipolar field of all other dots. This can be measured on global hysteresis loops of the arrays [Figs. 1(b) and 1(c)]. From the difference between fully saturated and remnant magnetization (3% in LDA and 5% in HDA), we can estimate a total width of the weakly magnetic parts along the lines at about 60 and 100 nm, respectively, for the LDA and HDA.

The presence of these weakly magnetic areas around the dots is crucial to our study, since it ensures that the nucleation is always initiated at low fields at the dot boundaries. The full reversal of the magnetization in each dot, at a switching field H_s, is then controlled only by the local values of both the DW propagation field H_p and the dipolar field H_d. This behavior contrasts markedly with that exhibited for dots separated by etching [7,8].

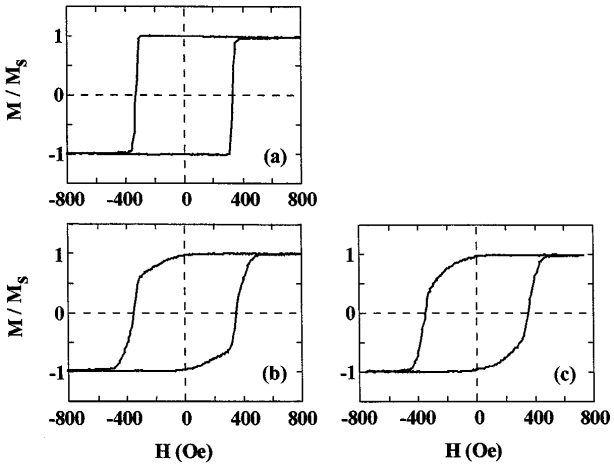

FIG. 1. Faraday hysteresis loops using a field sweeping rate of 64 Oe/s, for (a) the unpatterned part of the sample, (b) the LDA, and (c) the HDA.

Another important consequence of our FIB patterning method is that, since there is negligible etching, only very small optical contrast is observed between irradiated lines and dots. Faraday rotation MO microscopy [9] could then be used to monitor the magnetization reversal in the different parts of our sample, with a high resolution (0.5 μm) unhampered by diffraction effects.

In the unpatterned part, the magnetization reversal proceeds first by nucleation at the boundary of the arrays and then develops by uniform DW motion. This gives a very square hysteresis loop [Fig. 1(a)]. The weak pinning of DW results in a narrow Gaussian distribution of the propagation field [15], centered at $H_p = 323$ Oe and with variance $\Delta H_p \approx 20$ Oe, which confirms the good homogeneity of the film.

In dot arrays, we indeed observe that the reversal in low applied field H (<180 Oe) is initiated inside the irradiated lines, especially near corners of the dots. Magnetization then reverses in dots by DW motion when H becomes larger than the local switching field $H_s = H_p + H_d$. The dipolar field H_d depends on the local environment of the dots at each stage of the magnetization reversal of the array. In the first stages of the reversal, H_d favors the switching, and many dots are already reversed when the DW begins to propagate in the unpatterned part of the sample [Figs. 1(b) and 1(c)]. This is a direct proof of the efficiency of dipolar effects in the dot arrays. On the other hand, the switching of the last dots in the arrays is difficult since H_d becomes positive. Even more, due to the larger H_d values near the dot boundaries, the wall nucleated near the irradiated lines has first to overcome a large energy barrier before entering the central part of the dot. This explains the high-field tails

of the hysteresis loops found for the arrays [Figs. 1(b) and 1(c)], with a saturation field about 100 Oe higher than the coercive field of the unpatterned area [Fig. 1(a)], in good agreement with our dipolar field calculation.

The resolution and sensitivity of our MO microscopy allowed us to study in detail the switching of single dots. Contrary to isolated dots [1], single dot hysteresis loops are generally shifted with respect to $H = 0$. This means that the two local demagnetizing fields for "up" and "down" spin reversals differ from each other, due to different magnetic configurations of surround dots [6,7]. In order to illustrate this behavior, we have selected two single dot loops of the LDA, that of the first switching dot, starting from the down magnetically saturated state [Figs. 2(a) and 2(b)], and that of the last switching dot when all other dots are reversed [Figs. 2(c) and 2(d)]. Note that the coercive fields of Figs. 1 and 2 cannot be easily compared, as the two sets of experiments were performed over drastically different time scales. From the extreme values of the switching fields $H_s^{\min} = 230$ Oe [Fig. 2(a)] and $H_s^{\max} = 392$ Oe [Fig. 2(c)], one can estimate a mean switching field $\overline{H}_s = (H_s^{\min} + H_s^{\max})/2 = 311$ Oe, and a "dipolar field dispersion" $\Delta h_d = (H_s^{\min} - H_s^{\max})/2 = 81$ Oe. As discussed above, ΔH_d is far larger than the propagation field dispersion inside dots ($\Delta H_p \approx 20$ Oe) and comparable to the dipolar field values at their boundaries.

When the probed area ($1.1 \times 1.5\ \mu m^2$) overlaps the surrounding irradiated lines, the loops are rounded before showing a rapid jump [Figs. 2(a) and 2(c)], while they are highly square [Figs. 2(b) and 2(d)] when probing only the central part of the dot (over a $0.34 \times 0.45\ \mu m^2$ area).

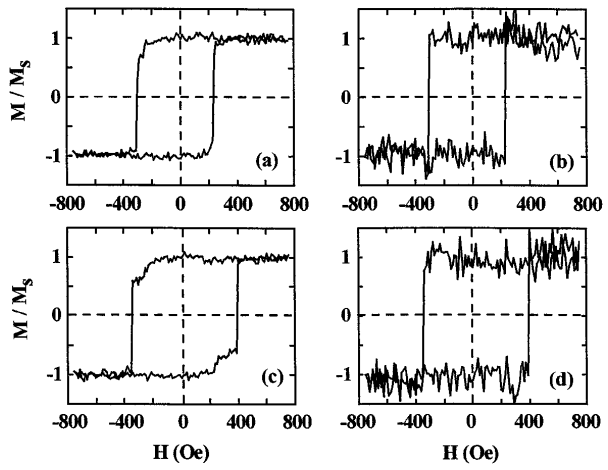

FIG. 2. Magnetic hysteresis loops measured on two selected dots of the LDA: (a) For a probed area of $1.1 \times 1.5\ \mu m^2$, the $H > 0$ jump corresponds to the reversal of one of the first dots of the array; (b) same dot but when probing its central area over $0.33 \times 0.45\ \mu m^2$; (c) for a probed area of $1.1 \times 1.5\ \mu m^2$, the $H > 0$ jump corresponds to the reversal of one of the last dots in the array; (d) same dot but when probing its central part over a $0.33 \times 0.45\ \mu m^2$ area.

This agrees with our interpretation above. For instance, the behavior of the dots reversing at high field [Fig. 2(c)] reflects the high nonuniformity of the dipolar field inside the dots: The magnetization is clearly stabilized before the jump, because the reversal initiated in the weakly magnetic areas near the boundaries is trapped by the larger dipolar field values at the dot borders.

Similar behaviors are observed also for the HDA, although with a weaker dipolar coupling strength and less square single dot hysteresis loops, as expected from the larger dot separation and wider weakly magnetic areas.

The checkerboard pattern, with adjacent single domain dots having antiparallel magnetization, stands as the most stable zero field configuration for an array of Ising dots with dipolar coupling. It is reasonable to assume that this equilibrium state can be approached through demagnetization by applying a slowly varying perpendicular ac magnetic field with a triangular shape of decreasing amplitude. Low amplitude decrease (4.54 Oe between two successive extremes) and field sweeping rate (2.28 Oe/s) were chosen, after checking that similar patterns are obtained for slower rates.

Figure 3 shows the magnetic configuration of the two arrays in their final demagnetized state. One observes rather large checkerboard regions, but linked by small portions of stripes or disordered zones. This looks similar to antiphase or twinned boundaries in crystals or nematics.

Quantitative topological information can be obtained by determining the proportion N_1 (N_2) of dots with opposite (identical) spin orientation for nearest neighbor (next-nearest neighbor) dots. N_1 and N_2 values and their standard deviation for eight identical demagnetization processes are reported in Table I for the two arrays. Large N_1 and N_2 values (close to 1) indicate a strong dipolar interaction, while $N_1 = N_2 = 0.5$ are expected for noninteracting particles. The HDA shows lower values of N_1 and N_2 than the LDA, which is consistent with the less perfect checkerboard state displayed in Fig. 3(b), in agreement with a smaller dipolar coupling in the HDA.

Model numerical simulations of the demagnetization process were performed on an array of 25×25 square Ising spins i. A narrow Gaussian distribution $H_{p,i}$ of intrinsic switching fields is used to map the experimental spread of propagation fields. Moreover, every cell is

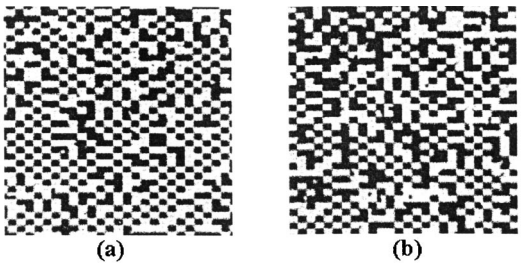

FIG. 3. Demagnetized states for the (a) LDA and (b) HDA (image area $34.6 \times 34.6\ \mu m^2$).

TABLE I. R, N_1, and N_2 parameters measured on the demagnetized states of experimental arrays and simulations.

	R	N_1	N_2
LDA	4.1	0.750(0.004)	0.655(0.004)
HDA	···	0.682(0.008)	0.58(0.01)
	0	0.501(0.007)	0.499(0.004)
Numerical	0.44	0.524(0.006)	0.500(0.005)
simulations	4.4	0.746(0.004)	0.636(0.005)
	44	0.930(0.005)	0.879(0.008)

submitted to a dipolar field $H_{d,i} = \sum_{j \neq i}(-\sigma/r_{ij}^3)$, where σ is the dipolar coupling strength. The magnetic field is changed by steps, and only a fraction of the cells i are switched at each step, according to the Néel-Brown probability of reversal $p_i = 1 - \exp(-t/\tau_i)$ with $\tau_i = \tau_0 \exp(\Delta E_i/kT)$. t represents the time between field steps, and ΔE_i is proportional to $(H_{p,i} + H_{d,i} - H)$, with $p_i = 1$ when $H > H_{p,i} + H_{d,i}$ [16]. The dipolar contributions were summed over five coordination shells, after checking that summation over 18 coordination shells leads to N_1 and N_2 values smaller by only 0.01. The dipolar field dispersion ΔH_d is determined from the difference between the coercive field of the whole array and the switching field of the first reversed dot.

Our simulations clearly show that the frustrated zones between checkerboard areas originate from the competition between dipolar coupling and dispersion of H_p. Magnetic mismatch occurs at the coalescence of checkerboard regions randomly nucleated from a few dots having the highest H_p values: These are the first to become stable during demagnetization. So the ratio $R = \Delta h_d/\Delta H_p$ is a crucial parameter. Simulated images of demagnetized states for increasing values of R are shown in Fig. 4. The

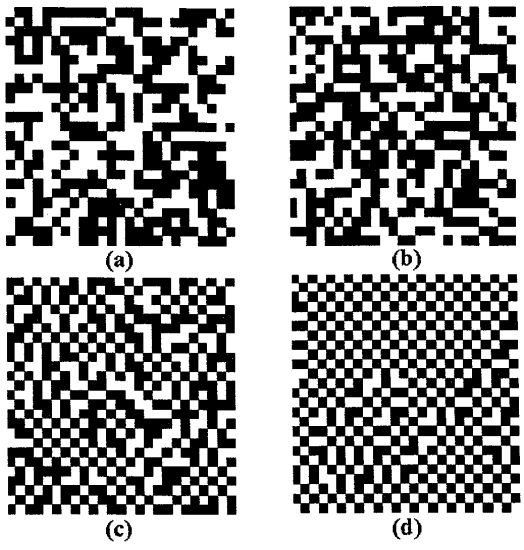

FIG. 4. Simulation results of the demagnetized states for different strengths of the dipolar coupling: (a) $R = 0$; (b) $R = 0.44$; (c) $R = 4.4$; (d) $R = 44$.

corresponding values of N_1 and N_2 are reported in Table I. As expected, more and more nearest neighbor dots have antiparallel magnetization as R is increased. Note the surprisingly good agreement between experimental data for the LDA and simulation with $R = 4.4$, close to the experimental value $R_{\mathrm{LDA}} \approx 4.1$.

In conclusion, starting from a Co/Pt ultrathin film structure and using an original FIB irradiation technique we succeeded in fabricating arrays of perpendicularly magnetized dots with clear dipolar coupling effects. From a comprehensive MO microscopy study, coupled to numerical simulations, we arrived at a detailed understanding of the parameters which drive the single dot and collective magnetization reversal behaviors, as, for instance, the formation of magnetostatically frustrated zones in the arrays. Such systems can be regarded as ideal models for understanding the influence of dipolar interactions on the magnetization reversal in media with perpendicular anisotropy. Our work opens also new possibilities to study other phenomena such as frustration effects in organized systems.

This work was made within the ISARD Collaboration (Université d'Orsay) and the SUBMAGDEV European TMR network and funded under CNRS-Ultimatech grants.

*On leave from Institut für Experimentelle und Angewandte Physik, Universität Regensburg (Germany).

[1] Jian-Gang Zhu and H. Neal Bertram, J. Appl. Phys. **66**, 1291 (1989).
[2] F. Schmidt and A. Hubert, J. Magn. Magn. Mater. **61**, 307 (1986).
[3] Li Cheng-Zhang and J. C. Lodder, J. Magn. Magn. Mater. **88**, 236 (1990).
[4] E. O. Samuel *et al.*, J. Magn. Magn. Mater. **115**, 327 (1992).
[5] A. Maeda *et al.*, J. Appl. Phys. **76**, 6667 (1994).
[6] M. Pardavi-Horvath and G. Vertesy, IEEE Trans. Magn. **MAG-30**, 124 (1994).
[7] M. Pardavi-Horvath, IEEE Trans. Magn. **MAG-32**, 4458 (1996).
[8] J.-P. Jamet *et al.*, Phys. Rev. B **57**, 14 320 (1998).
[9] J. Pommier *et al.*, Phys. Rev. Lett. **65**, 2054 (1990).
[10] R. F. C. Farrow *et al.*, J. Cryst. Growth **133**, 47 (1993).
[11] S. Lemerle *et al.*, Phys. Rev. Lett. **80**, 849 (1998).
[12] N. W. E. McGee *et al.*, J. Appl. Phys. **73**, 3418 (1993).
[13] C. Chappert *et al.*, Science **280**, 1919 (1998).
[14] G. Ben Assayag *et al.*, J. Vac. Sci. Technol. B **11**, 2420 (1993).
[15] J. Ferré *et al.*, Phys. Rev. B **55**, 15 092 (1997).
[16] The simulations were made using experimental parameters determined on similar ultrathin films [A. Kirilyuk, J. Ferré, and D. Renard, Europhys. Lett. **24**, 403 (1993)]. Only very few dots are concerned by thermal activation in a demagnetizing process, and the results are not very sensitive to the set of parameters.